Journal of Magnetic Resonance **140,** 347–350 (1999)
Article ID jmre.1999.1831, available online at http://www.idealibrary.com on IDEAL®

Simple but Reliable Solutions for Spiral MRI Gradient Design

C. Salustri,* Y. Yang,† and G. H. Glover‡

*Institute of Solid State Electronics, CNR, Rome, Italy I-00156; †Laboratory for Diagnostic Radiology Research, OD/NIH, Bethesda, Maryland 20892; and ‡Department of Diagnostic Radiology, Lucas MRI Center, Stanford University School of Medicine, Stanford, California 94305-5488

Received October 17, 1998; revised May 10, 1999

The efficiency of gradient design in MRI is limited by the simple fact that the gradient coil current and slew rate cannot exceed hardware threshold values. In spiral MRI, which requires gradients to be very rapidly switched between positive and negative values, minimization of the acquisition time is achieved by maintaining the current and slew rate as high as possible during the entire measurement. Since the current and slew rate compete against each other, an efficient gradient design consists of two parts in which current and slew rate are pushed alternatively to their limits. Values for these types of gradients can be obtained by solving numerically the equation of motion for the spiral trajectory. This paper shows that simple but reasonable mathematical approximations deliver reliable analytical solutions. Images obtained using these analytical solutions do not show evident distortions when compared with images obtained with numerical solutions.

Key Words: **spiral MRI; fast imaging; magnetic resonance imaging.**

INTRODUCTION

Many situations exist in MRI where fast image acquisition is of particular importance; very old or very young subjects (*1, 2*), for example, find it rather difficult to stay still as do many psychiatric patients (*3*). Other examples include cardiac imaging (*4, 5*), studies of flow dynamics (*6*), or studies of development of hemoglobin oxygenation (functional MRI) (*7*). For this reason, many sequences have been proposed in the past few years to reduce the length of the acquisition window (*8–13*), a task which is far from easy, since gradient waveforms must be designed in such a way that the desired trajectory in k space is properly traced without exceeding the limitations of the hardware in use. Hardware constraints limit primarily two parameters: the gradient amplitude (which is limited by the peak current of the amplifier) and the gradient slew rate (which is limited by how fast the hardware can change the instantaneous gradient value). Spiral MRI (*14–19*) has recently acquired increasing importance among the fast MRI sequences since it is softer on the hardware, but still provides excellent SNR and good robustness against motion. As the name suggests, the k space is traced with a spiraling trajectory, which avoids the sharp gradient switching typically necessary in the "raw after raw" acquisitions such as EPI. On the other hand, spiral MRI suffers from image blurring, caused by phase accrual related to off-resonance spins. If we define the vector $\mathbf{k}$ in k space as

$$k_x = |\mathbf{k}|\cos\,\theta \qquad [1a]$$

$$k_y = |\mathbf{k}|\sin\,\theta \qquad [1b]$$

with $\theta = (2\pi n/T)\,f(t)$, then the tip of $\mathbf{k}$ traces an Archimedean spiral if $|\mathbf{k}(t)| = A\theta$, where $A = 1/(2\pi\mathrm{FOV})$ is constant. Since $\mathbf{k} = (\gamma/2\pi)\int_0^t \mathbf{g}(t')dt'$, where $\mathbf{g}(t')$ is the gradient vector, then optimal gradient waveforms can be determined by solving the equations of motion of $\mathbf{k}$. Exact solutions of the differential equations of motion resulting from Eqs. [1] can be obtained only with numerical methods. We show here that simple approximations can provide reliable analytical solutions, and that gradient waveforms accordingly designed provide uniform and time efficient coverage of k space while maintaining accurate image quality.

METHOD

The time evolution of the gradient follows simply from the time derivative of $\mathbf{k}$,

$$g_x = (2\pi/\gamma)A\dot{\theta}(\cos\,\theta - \theta\,\sin\,\theta) \qquad [2a]$$

$$g_y = (2\pi/\gamma)A\dot{\theta}(\sin\,\theta + \theta\,\cos\,\theta) \qquad [2b]$$

and the expression of the slew rate follows as the time derivative of the gradient:

$$s_x = (2\pi/\gamma)A[(\ddot{\theta} - \theta\dot{\theta}^2)\cos\,\theta - (2\dot{\theta}^2 + \theta\ddot{\theta})\sin\,\theta] \qquad [3a]$$

$$s_y = (2\pi/\gamma)A[(\ddot{\theta} - \theta\dot{\theta}^2)\sin\,\theta + (2\dot{\theta}^2 + \theta\ddot{\theta})\cos\,\theta]. \qquad [3b]$$

Our aim was to find time efficient analytical solutions of these differential equations. The fastest spiral in k space would be traced with x and y gradient components which, both starting from zero, oscillate with an amplitude and phase such that the resulting vector $\mathbf{g}$ reaches immediately its maximum modulus

1090-7807/99 $30.00

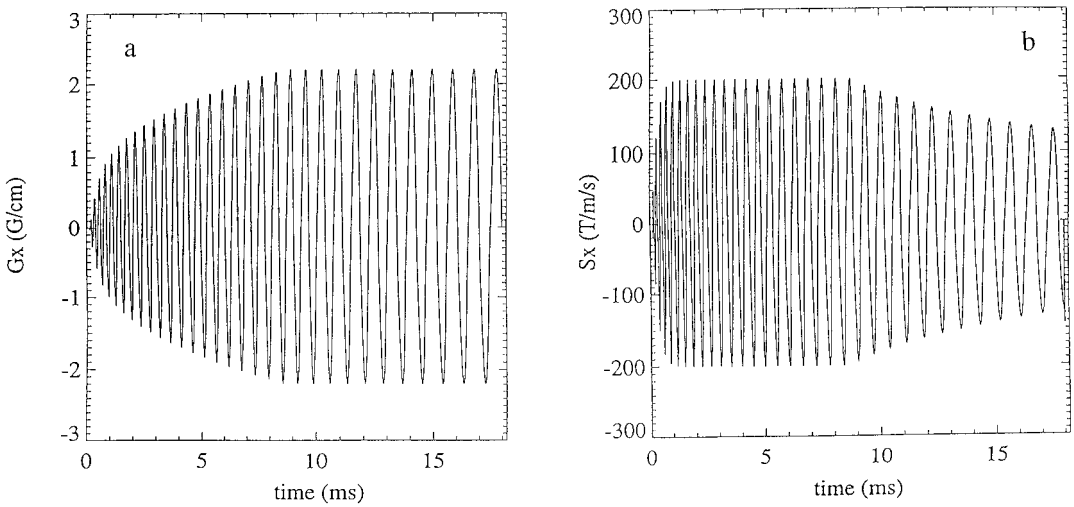

FIG. 1. Plot of the gradient amplitude (a) generated by the "two-part" analytical solutions of the spiral equations of motion and of the corresponding slew rate (b) (only x components are shown). The link between the "maximum slew rate" and the "maximum amplitude" regimes is at about 8.5 ms after the onset.

and remains constant from then on. This is impossible in practice, though, since for the gradient to have a constant amplitude throughout the entire acquisition window, its components would have to oscillate very fast when tracing the spiral near the center of k space: the slew rate of these oscillations would be consequently exceedingly high. In a similar way a gradient whose time evolution is characterized by a constant and maximum slew rate would require exceedingly high amplitude values when tracing the periphery of k space. This problem can be circumvented by means of a gradient waveform made of two parts (*20*): a first part characterized by a constant slew rate, applied until the amplitude reaches its maximum allowed value, and a second part, with constant amplitude, which starts near the time when the slew rate falls below its maximum allowed value and ends when θ has completed the desired number of turns. We obtain a constant slew rate gradient waveform from Eqs. [3] by imposing

$$|\mathbf{s}| = [s_x^2 + s_y^2]^{1/2} = (2\pi/\gamma) A[(\ddot{\theta} - \theta\dot{\theta}^2)^2 + (2\dot{\theta} + \theta\ddot{\theta})^2]^{1/2} = s_{\max}. \quad [4]$$

Assuming $\ddot{\theta}$ much smaller than $\dot{\theta}^2$ for most of the trajectory, and in the approximation $\theta^2 \gg 1$, Eq. [4] has a simple analytical solution:

$$\theta = \left[\frac{3}{2}\left(\frac{\gamma s_{\max}}{2\pi A}\right)^{1/2} t\right]^{2/3}. \quad [5]$$

In a similar way, we obtain a constant amplitude gradient from Eqs. [3] by imposing

$$|\mathbf{g}| = [g_x^2 + g_y^2]^{1/2} = (2\pi/\gamma) A\dot{\theta}[1 + \theta^2]^{1/2} = g_{\max}, \quad [6]$$

which, again for $\theta^2 \gg 1$, also has a simple analytical solution:

$$\theta = \left[\left(\frac{\gamma g_{\max}}{\pi A}\right) t\right]^{1/2}. \quad [7]$$

We generated our two-part gradient waveform simply by substituting in Eqs. [2] θ given by Eq. [5] for the first part (slew rate limited) and θ given by Eq. [7] for the second part (amplitude limited). $g_{\max}$ and $s_{\max}$ were set by the hardware characteristics of our 1.5-T GE SIGNA (General Electric, Milwaukee, WI) scanner. Nonetheless, to obtain the final gradient design, two important points had to be addressed: (a) the link between the two parts and (b) the gradient waveform when tracing the center of k space, where the approximation $\theta^2 \gg 1$ does not hold.

An accurate link of the two parts is fundamental since any dramatic discontinuity in the slope of the final gradient waveform would cause inhomogeneity in tracing the k space. On the other hand, Eqs. [5] and [7] show that θ has completely different time evolutions in the two cases of constant slew rate and constant gradient: this means that the slopes of the two waveforms at the time points when they cross their respective thresholds almost certainly will differ enough to cause a visible discontinuity at the point of linkage. In order to find a proper linkage we computed the slopes of the slew rate limited waveform at all time points within the one period of oscillation immediately preceding its threshold crossing and the slopes of the gradient-limited waveform at all time points within the one period immediately following its threshold crossing. Time points were 4 μs apart, which was our scanner's sampling resolution. The two waveforms were linked at the points at

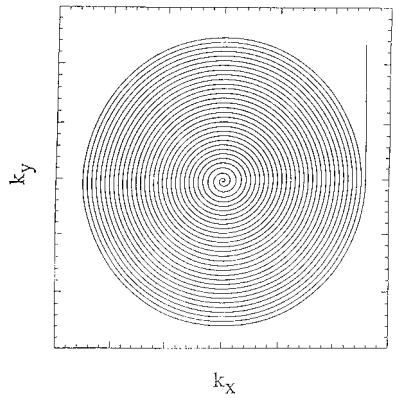

FIG. 2. *k*-space trajectory designed for a 64 × 64 equivalent matrix size with 240 mm FOV corresponding to the two-part gradient design shown in Fig. 1.

which the difference between the slopes of the two waveforms was at a minimum, i.e., at the points which provided the smoothest amplitude transition from one regime to the other.

In addition, special attention had to be given to the gradient waveform in the vicinity of $t = 0$, where the approximation $\theta^2 \gg 1$ obviously does not hold. In fact, due to the presence of the time derivative of θ in the gradient expression, the substitution of Eq. [5] into Eq. [2] results in the appearance of the variable t in the denominator, which causes the gradient waveform to exceed the slew rate limit for $t \sim 0$ and to diverge at $t = 0$. We modulated the amplitude of the gradient waveform in the vicinity of $t = 0$ with the function $1 - \exp(-t/\tau)$, choosing τ such as to keep the gradient slew rate below its limit. In particular in the present study, we chose a value of τ which allowed the gradient amplitude to increase from zero following the profile assumed by the waveform for $t \gg 0$ (see Fig. 1a). As shown in Fig. 1b, this choice generated a rather overconservative slew rate, well below its limit during approximately the first millisecond. It is useful to note that from a computational point of view, both the proper linkage and the modulation of the gradient amplitude were easily obtained by means of a few extra statements in the program generating the gradient waveforms. In this way we generated x and y components of

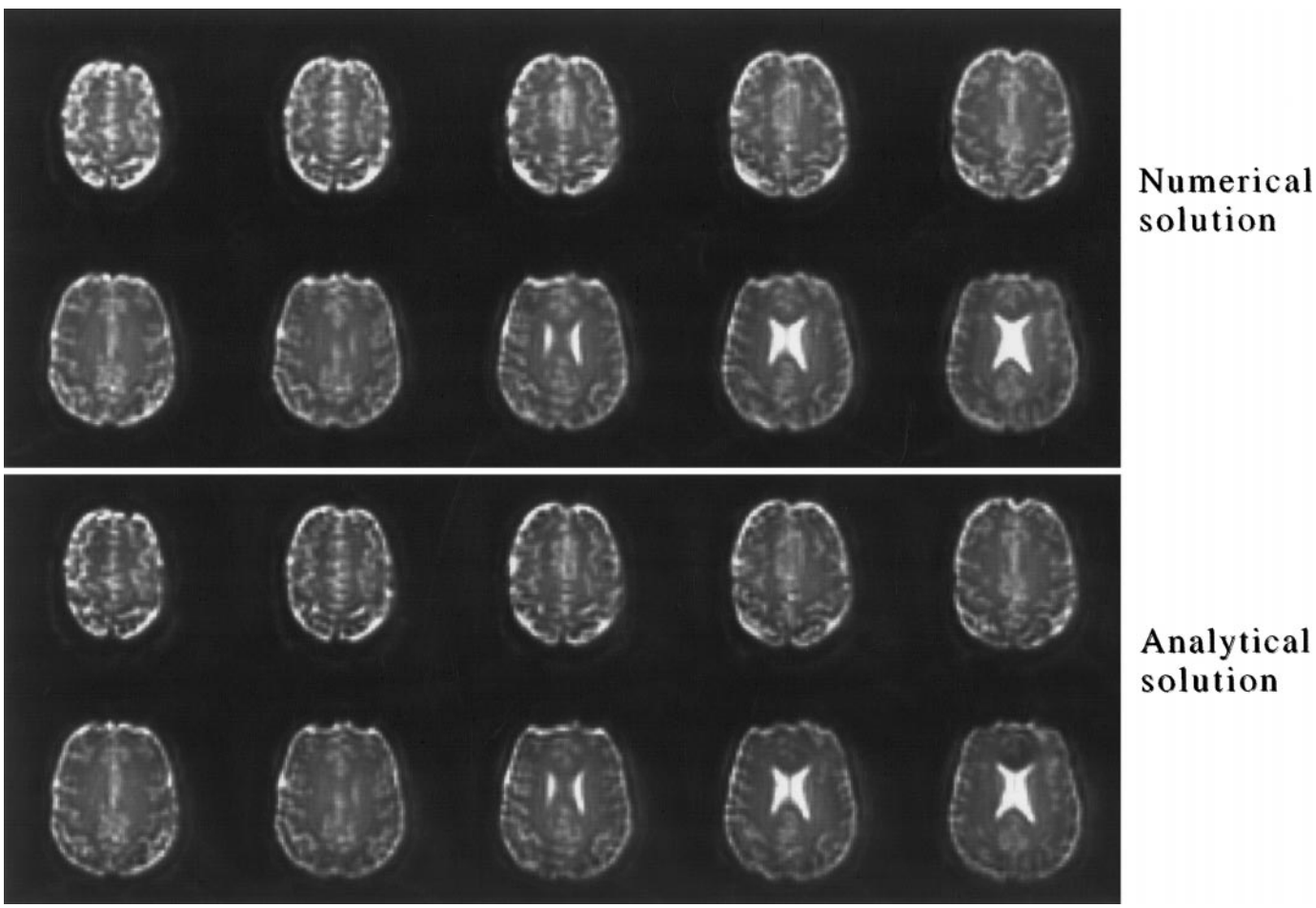

FIG. 3. Comparison between two equivalent series of axial scans of the same brain obtained at 1.5 T with the spiral sequence described in the paper. The two sets were obtained using respectively the numerical (upper) and analytical (lower) solutions of the equation of motion for the spiral trajectory.

the vector **g** that, starting from zero, increase their amplitudes with a constant maximum slew rate (200 T/m/s) until the maximum allowed amplitude (22 mT/m) is reached; from this point on the gradient waveform continues with constant amplitude and below-maximum, decreasing slew rate. Figures 1a and 1b show this behavior for the *x* component of both gradient amplitude and slew rate. It can be seen that the link is at about 8.5 ms after the onset. Figure 2 shows the resulting spiral trajectory in *k* space designed for a 64×64 equivalent matrix size with 240 mm FOV.

RESULTS

We applied these analytical solutions to imaging of the brain of one subject and compared the results with images of the same brain taken with a two-part design of the gradients but generated from numerical integration (Runge–Kutta) of the equation of motion. Figure 3 shows this comparison. The study was part of a board-approved intramural research protocol of the National Institutes of Health. Our focus was to see if the above-described approximations would cause image distortions and would affect the robustness of these solutions against motion. The resulting images were indeed very similar. It could be noted that the subject was probably very still, being one of the authors and consequently substantially motivated. The outstanding similarity of the two sets of images also encourages us to believe that our procedure can be useful when the acquisition duration is a concern: in fact, in this case further manipulation of the gradient waveform in the vicinity of $t = 0$ could reduce redundancy in the center of *k* space, where numerical solutions of the equation of motion notoriously produce oversampling. This would result in an increase in the acquisition speed.

ACKNOWLEDGMENTS

The authors are grateful to Jeff Duyn for the many helpful discussions and to Joseph A. Frank for his continuous supervision and encouragement.

REFERENCES

1. R. Raininko, T. Autti, S. L. Vanhanen, A. Ylikoski, T. Erkinjuntti, and P. Santavuori, *Neuroradiology* **36**(5), 364 (1994).
2. O. Salonen, T. Autti, R. Raininko, A. Ylikoski, and T. Erkinjuntti, *Neuroradiology* **39**(8), 537 (1997).
3. D. R. Weinberger, V. Mattay, J. Callicott, K. Kotrla, A. Santha, P. van Gelderen, J. Duyn, C. Moonen, and J. A. Frank, *Neuroimage* **4,** S118 (1996).
4. J. H. Grollman Jr., *Cathet. Cardiovasc. Diagn.* **42**(2), 208 (1997).
5. P. Croisille and D. Revel, *J. Belge Radiol.* **80**(3), 133 (1997).
6. R. H. Mohiaddin, P. D. Gatehouse, M. Henien, and D. N. Firmin, *J. Magn. Reson. Imaging* **7**(4), 657 (1997).
7. S. Ogawa, T. M. Lee, A. R. Kay, and D. W. Tank, *Proc. Natl. Acad. Sci. USA* **87,** 9868 (1990).
8. M. Reiser and S. C. Faber, *Eur. Radiol.* **7**(14), 166 (1997).
9. F. Schick, *Magn. Reson. Med.* **38**(4), 638 (1997).
10. M. R. Patel, R. A. Klufas, R. A. Alberico, and R. R. Edelman, *Am. J. Neuroradiol.* **18**(9), 1635 (1997).
11. D. K. Sodickson and W. J. Manning, *Magn. Reson. Med.* **38**(4), 591 (1997).
12. S. Trattnig, M. Breitenseher, G. Kontaxis, T. Helbich, T. Rand, and H. Imhof, *Acta Radiol.* **38**(5), 880 (1997).
13. E. R. Melhem, H. Jara, H. Shakir, and T. A. Gagliano, *Am. J. Neuroradiol.* **18**(9), 1627 (1997).
14. C. H. Meyer, B. S. Hu, D. G. Nishimura, and A. Macovski, *Magn. Reson. Med.* **28,** 202 (1992).
15. G. Nishimura, P. Irarrazabal, and C. H. Meyer, *Magn. Reson. Med.* **33,** 549 (1995).
16. D. C. Noll, J. D. Cohen, C. H. Meyer, and W. Schneider, *J. Magn. Reson. Imaging* **5,** 49 (1995).
17. G. H. Glover and A. T. Lee, *Magn. Reson. Med.* **33,** 624 (1995).
18. Y. Yang, G. H. Glover, P. van Gelderen, V. S. Mattay, K. S. Attanagoda Santha, C. T. W. Moonen, D. R. Weinberger, J. A. Frank, and J. H. Duyn, *Magn. Reson. Med.* **36,** 620 (1996).
19. J. H. Duyn and Y. Yang, *J. Magn. Reson.* **128,** 130 (1997).
20. K. F. King, K. F. F. Foo, and C. R. Crawford, *Magn. Reson. Med.* **34,** 156 (1995).